Towards exact subgrid-scale models for explicitly filtered large-eddy simulation of wall-bounded flows

By H. J. Bae AND A. Lozano-Durán

1. Motivation and objectives

The equations for large-eddy simulation (LES) are formally derived by applying a low-pass filter to the Navier–Stokes (NS) equations (Leonard 1975). Typically, no explicit filter form is specified, and the discrete differentiation operators act as an effective implicit filter. The resulting velocity field is then assumed to be representative of the filtered velocity. However, although the discrete operators have a low-pass filtering effect, the associated filter acts only in the single spatial direction in which the derivative is applied (Lund 2003), and thus each term in the NS equations takes on a different filter form. In addition, numerical errors and the frequency content are difficult to control for the implicit filter approach, and the solutions are grid dependent (Kravchenko & Moin 2000; Meyers & Sagaut 2007).

Another important limitation of implicitly filtered LES is the known fact that the subgrid scale (SGS) tensor does not coincide with the Reynolds stress terms resulting from filtering the NS equations due to the implicit filter operator. This ambiguity renders DNS inadequate for the development of SGS models. On the contrary, when the filter operator is well defined and consistent with the filtered NS (fNS) equations, DNS data provides the necessary information to construct exact SGS models, as demonstrated by De Stefano & Vasilyev (2002) for the simple Burger's equation. In order to exploit the rich amount of DNS data as a tool to devise SGS models, it is indispensable to provide an LES framework consistent with the fNS equations, that is, explicitly filtered LES.

Previous works on explicitly filtered LES include the study of Winckelmans *et al.* (2001), who investigated a two-dimensional explicitly filtered isotropic turbulence and channel flow LES to evaluate various mixed subgrid/subfilter scale models. Stolz *et al.* (2001) implemented the three-dimensional filtering schemes of Vasilyev *et al.* (1998) by using an approximate deconvolution model for the convective terms in the LES equations. Lund (2003) applied two-dimensional explicit filters to a channel flow and evaluated the performance of explicitly filtered versus implicitly filtered LES. Gullbrand & Chow (2003) attempted the first grid-independent solution of the LES equations with explicit filtering. Bose *et al.* (2010) further investigated the grid independence of explicitly filtered LES with a three-dimensional filter for turbulent channel flows.

All previous investigations of wall-bounded explicitly filtered LES retain some inconsistencies with the rigorously derived incompressible fNS equations. In Lund (2003) and Gullbrand & Chow (2003), the filter operator in the wall-normal direction was implicit even though the grid resolution was too coarse to elude the use of a filter. In Vasilyev *et al.* (1998) and Bose *et al.* (2010), the filter size varied as a function of the wall-normal distance, and the divergence-free condition for incompressible flows was only satisfied up to a prescribed order of accuracy.

In this study, we present a formulation of the incompressible fNS equations maintaining consistency between the continuity equation, the filter operator, and the boundary conditions at the wall. Our analysis is focused on the formulation of fNS equations in the limit of continuous space. An important observation in this case is that there is no closure problem, provided that the filter operator is reversible. Nonetheless, the resolution requirements for the discretized fNS equations are similar to those for the unfiltered NS equations, and when the grid resolution is insufficient to resolve all scales of turbulence, SGS models are required to supply the contribution from the irreversibly lost scales below the grid cutoff (Carati *et al.* 2001). Despite the fact that the fNS equations are as demanding as the NS equations in terms of resolution requirements, the formulation of consistent fNS equations is advantageous to inform SGS models for explicitly filtered LES.

The report is organized as follows. In Section 2, the fNS equations are introduced, and their solution is compared to the solution of the unfiltered equations for isotropic turbulence. In Section 3, we discuss the difficulty of formulating consistent fNS equations for wall-bounded flows and provide a solution for flows over flat walls. Finally, conclusions are offered in Section 4.

2. Filtered Navier–Stokes equations

The incompressible NS equations and for momentum and mass conservation are

$$\frac{\partial u_i}{\partial t} + \frac{\partial u_i u_j}{\partial x_j} = -\frac{1}{\rho}\frac{\partial p}{\partial x_i} + \nu \frac{\partial^2 u_i}{\partial x_j \partial x_j}, \quad \frac{\partial u_i}{\partial x_i} = 0, \tag{2.1}$$

where u_i are the velocity components, ρ is the fluid density, ν is the kinematic viscosity, and p is the pressure. The filter operator on a variable ϕ in integral form is defined by

$$\bar{\phi}(\boldsymbol{x}) \equiv \mathcal{F}(\phi)(\boldsymbol{x}) = \int_\Omega G(t, \boldsymbol{x}, \boldsymbol{x'})\phi(\boldsymbol{x'})\mathrm{d}\boldsymbol{x'}, \tag{2.2}$$

where $\boldsymbol{x} = (x_1, x_2, x_3)$, G is the filter kernel, and Ω is the domain of integration. When Eq. (2.1) is filtered with Eq. (2.2), the resulting equations are

$$\overline{\frac{\partial u_i}{\partial t}} + \overline{\frac{\partial u_i u_j}{\partial x_j}} = -\frac{1}{\rho}\overline{\frac{\partial p}{\partial x_i}} + \nu \overline{\frac{\partial^2 u_i}{\partial x_j \partial x_j}}, \quad \overline{\frac{\partial u_i}{\partial x_i}} = 0. \tag{2.3}$$

The filter and differentiation operators commute when the kernel of the filter is invariant under translation in space and time, that is, $G(t, \boldsymbol{x}, \boldsymbol{x'}) = G(\boldsymbol{x'})$. When this condition is satisfied, Eq. (2.3) can be rewritten as

$$\frac{\partial \bar{u}_i}{\partial t} + \frac{\partial \overline{u_i u_j}}{\partial x_j} = -\frac{1}{\rho}\frac{\partial \bar{p}}{\partial x_i} + \nu \frac{\partial^2 \bar{u}_i}{\partial x_j \partial x_j}, \quad \frac{\partial \bar{u}_i}{\partial x_i} = 0, \tag{2.4}$$

which is valid for both reversible ($\mathcal{F}^{-1}$ exists) and irreversible filters. For reversible filters, since no information is lost, the term $\overline{u_i u_j}$ can be expressed as a function of $\bar{u}_i$. For symmetric filters with Fourier transform of class $\mathcal{C}^\infty$ the explicit form of $\overline{u_i u_j}$ as a function of $\bar{u}_i$ has been extensively studied by Yeo (1987), Leonard (1997) and Carati *et al.* (2001), among others. In these cases, Eq. (2.4) can be solved independently of Eq. (2.1) (no closure is required), and the solution of Eq. (2.1), u_i, is identical to the unfiltered solution of Eq. (2.4), denoted by $\mathcal{F}^{-1}(\bar{u}_i)$. For the remainder of the paper, we will focus on reversible filter operators.

2.1. *Exact SGS models for explicitly filtered LES*

In this section, we motivate how explicitly filtered LES with a consistent set of fNS equations can benefit from DNS data. When the equations are numerically integrated, another operator is introduced, i.e., numerical discretization. An in-depth analysis of the filter and discretization operators can be found in the work by Carati *et al.* (2001). If we denote the discretization operator by $\tilde{(\cdot)}$ and assume it commutes with the differentiation operator, the discrete fNS equations become

$$\frac{\partial \tilde{\bar{u}}_i}{\partial t} + \frac{\partial \widetilde{\overline{u_i u_j}}}{\partial x_j} = -\frac{1}{\rho}\frac{\partial \tilde{\bar{p}}}{\partial x_i} + \nu \frac{\partial^2 \tilde{\bar{u}}_i}{\partial x_j \partial x_j}. \tag{2.5}$$

The convective term of Eq. (2.5) is usually expressed in terms of the discrete filtered velocities and such that

$$\frac{\partial \tilde{\bar{u}}_i}{\partial t} + \frac{\partial \widetilde{\tilde{\bar{u}}_i \tilde{\bar{u}}_j}}{\partial x_j} = -\frac{1}{\rho}\frac{\partial \tilde{\bar{p}}}{\partial x_i} + \nu \frac{\partial^2 \tilde{\bar{u}}_i}{\partial x_j \partial x_j} - \frac{\partial \widetilde{\mathcal{T}_{ij}}}{\partial x_j}, \tag{2.6}$$

where $\mathcal{T}_{ij} = \overline{u_i u_j} - \tilde{\bar{u}}_i \tilde{\bar{u}}_j$. With an additional assumption that filter and the discretization operators are commutative, this can be further decomposed as

$$\mathcal{T}_{ij} \equiv \overline{u_i u_j} - \tilde{\bar{u}}_i \tilde{\bar{u}}_j = \underbrace{(\overline{u_i u_j} - \overline{\tilde{u}_i \tilde{u}_j})}_{\overline{\mathcal{A}_{ij}}} + \underbrace{(\overline{\tilde{u}_i \tilde{u}_j} - \tilde{\bar{u}}_i \tilde{\bar{u}}_j)}_{\mathcal{B}_{ij}}. \tag{2.7}$$

If the discretization errors are negligible (e.g., fine grid resolutions/DNS), then $\tilde{u}_i \approx u_i$ and $\mathcal{A}_{ij} \approx 0$. Thus, $\mathcal{A}_{ij}$ represents the errors due to discretization (grid resolution) and is accordingly named the SGS stress tensor. For the remainder of the paper, the discretization operator is omitted for DNS results. The term $\mathcal{B}_{ij}$ only depends on $\bar{\bar{u}}_i$, and it is known for reversible filters. Moreover, if there is no explicit filter, $\mathcal{B}_{ij} = 0$ and, subsequently, $\mathcal{B}_{ij}$ is called the subfilter scale (SFS) stress tensor. Note that only the term $\mathcal{A}_{ij}$ needs to be modeled since $\mathcal{B}_{ij}$ is only a function of the discretized velocities. Another important remark is that, given a numerical discretization, identical resolutions are demanded to integrate the NS and fNS equations with the same degree of accuracy. The reason can be found in the $u_i u_j$ term in $\mathcal{A}_{ij}$, which needs to be accurately computed in both cases and becomes the limiting factor for both equations.

One possible way of informing models for $\mathcal{A}_{ij}$ is by using DNS data. In the most extreme case, a exact SGS model can be produced by running a DNS in parallel with the equivalent initial condition. By assuming that the numerical errors are negligible for the DNS velocity field, the term $\mathcal{A}_{ij}$ can be evaluated as follows:

1. Using the DNS velocity field, $u_i u_j$ is computed.
2. The unfiltered discretized velocities from a explicitly filtered LES, $\tilde{u}_i$ are obtained by reversing $\mathcal{F}$, $\tilde{u}_i = \mathcal{F}^{-1}(\tilde{\bar{u}}_i)$.
3. The term $\tilde{u}_i \tilde{u}_j$ is computed.
4. $\mathcal{A}_{ij}$ is calculated by filtering $u_i u_j - \tilde{u}_i \tilde{u}_j$.

In order to utilize the rich DNS data available as described in the process above, it is absolutely indispensable to have a consistent fNS equations for both unbounded and bounded domains.

2.2. *Application of the filtered Navier–Stokes equations to isotropic turbulence*

In unbounded flows, e.g., isotropic turbulence, the condition $G(t, \boldsymbol{x}, \boldsymbol{x'}) = G(\boldsymbol{x'})$ is trivially enforced by utilizing a filter with constant filter size and shape.

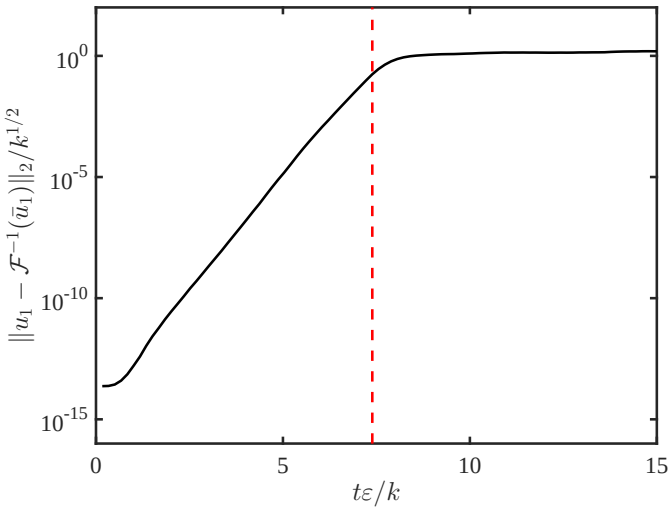

FIGURE 1. Error $\|u_1 - \mathcal{F}^{-1}(\bar{u}_1)\|_2$ as a function of $t\varepsilon/k$. Dashed line indicates $t\varepsilon/k = 7.39$.

Starting from the same initial conditions (filtered and unfiltered), the solutions u_i and $\bar{u}_i$ can be numerically obtained by discretizing their respective equations. However, the numerical errors will propagate and accumulate in time until the solutions diverge due to the chaotic nature of the NS equations. Despite the difference in u_i and $\mathcal{F}^{-1}(\bar{u}_i)$ for long times, both velocity fields are expected to be statistically equivalent if the error in the solutions is below a given tolerance for times longer than the auto-correlation time for the kinetic energy.

To quantify how the solutions of discretized NS and fNS equations diverge from one another, the error $\|u_1 - \mathcal{F}^{-1}(\bar{u}_1)\|_2$ for a DNS of forced isotropic turbulence is given as a function of time in Figure 1. The solutions were computed using the discrete Fourier transform in the three spatial directions with 256^3 modes in a triply-periodic domain of size $L^3 = (2\pi)^3$, and advancing in time with a fourth-order Runge-Kutta time-stepping. The filter operator selected is the differential filter from Germano (1986)

$$\bar{u}_i - a^2 \frac{\partial \bar{u}_i}{\partial x_j \partial x_j} = u_i \tag{2.8}$$

with $a^2/L^2 = 0.01$, where a is a characteristic filter size. This is equivalent to a filter with kernel

$$G(\boldsymbol{x}, \boldsymbol{x'}) = \frac{1}{4\pi a^2} \frac{\exp(-|\boldsymbol{x} - \boldsymbol{x'}|/a)}{|\boldsymbol{x} - \boldsymbol{x'}|}. \tag{2.9}$$

In this case, $\overline{u_i u_j}$ is directly given by

$$\overline{u_i u_j} = \overline{\left(\bar{u}_i - a^2 \frac{\partial \bar{u}_i}{\partial x_k \partial x_k}\right)\left(\bar{u}_j - a^2 \frac{\partial \bar{u}_j}{\partial x_k \partial x_k}\right)}. \tag{2.10}$$

The error is initially of machine precision and increases exponentially with time until it saturates after 8 integral time-scales, defined as k/ε, where k is the turbulent kinetic energy and ε is the energy dissipation rate. Note that the error is of the order of 10^{-6} (single precision) at $t \approx 5T_k$, where T_k is the auto-correlation time for the kinetic energy, which is reported to be ~ 1 integral time-scales (Cardesa *et al.* 2015). Figure 2 compares

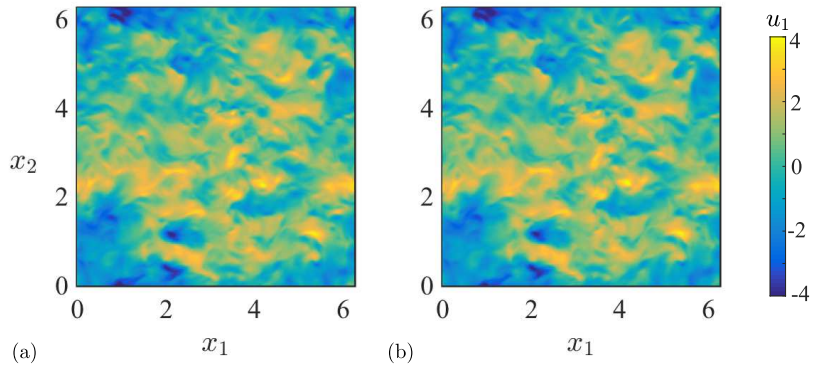

FIGURE 2. Instantaneous snapshot of (a) u_1 and (b) $\mathcal{F}^{-1}(\bar{u}_1)$ for the same x_1–x_2 plane at $t\varepsilon/k = 7.39$.

u_1 and $\mathcal{F}^{-1}(\bar{u}_1)$ at $t\varepsilon/k = 7.39$ for a fixed x_1–x_2 plane. The qualitative agreement between the two velocity fields is remarkable, despite the saturation of the quantitative discrepancy.

3. Filtered Navier–Stokes equations for wall-bounded flows

The preferred form of the fNS equations for practical applications is the one in Eq. (2.4), which requires the filter operator to commute with differentiation. This was successfully accomplished in Section 2.2 by using the differential filter with constant filter size, a^2, and periodic boundary conditions. However, unlike in unbounded flows, the presence of a wall imposes a limitation on the support of the kernel that violates the invariance of the filter under translation in space. If x_2 is the wall-normal direction, the kernel for Eq. (2.2) is inevitably of the form $G(x_2, \boldsymbol{x'})$ since the integration is bounded by the presence of the wall. Therefore, the filter and differentiation operators do not commute and Eq. (2.4) does not apply.

3.1. *Extension method*

For flat walls, we propose to resolve this limitation by extending the flow in the wall-normal direction, allowing for a uniform filter in the near-wall region as illustrated in Figure 3. From now on, we consider the flow over a smooth flat wall with x_1, x_2, and x_3 signifying the streamwise, wall-normal, and spanwise directions, respectively. Quantities evaluated at the wall, located at $x_2 = 0$, are denoted by $(\cdot)|_w$. The flow is then extended below the wall as

$$u_1(-x_2) = -u_1(x_2), \quad u_2(-x_2) = u_2(x_2), \quad u_3(-x_2) = -u_3(x_2), \tag{3.1}$$

where x_1 and x_3 are omitted for simplicity. In this manner, $\partial u_i/\partial x_i = 0$ is also satisfied in the extended domain, preserving incompressibility. The extension provided by Eq. (3.1) removes the limitation on the support of the kernel previously imposed by the wall, and Eq. (2.4) can be formally obtained for flows over flat walls. Note that, by symmetry, the filtered velocity field also satisfies

$$\bar{u}_1(-x_2) = -\bar{u}_1(x_2), \quad \bar{u}_2(-x_2) = \bar{u}_2(x_2), \quad \bar{u}_3(-x_2) = -\bar{u}_3(x_2). \tag{3.2}$$

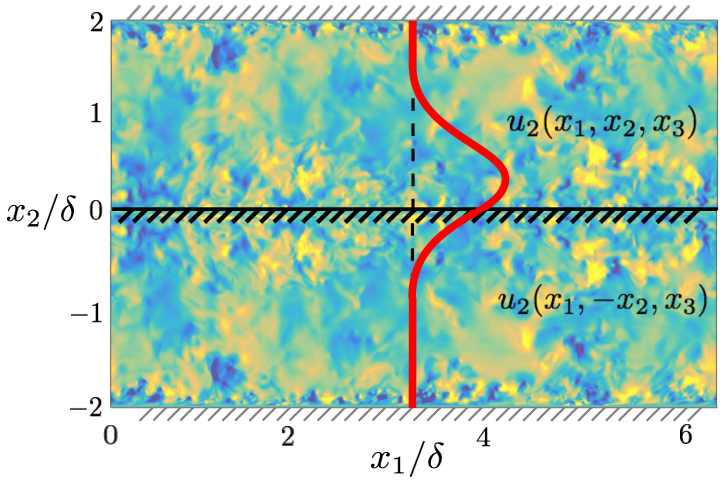

FIGURE 3. Illustration of the extension method in Eq. (3.1) for the wall-normal velocity component of a turbulent channel flow. Solid line depicts the kernel of the filter operator, which can extend beyond the wall.

Another possible extension consistent with the incompressibility condition is

$$u_1(-x_2) = u_1(x_2), \quad u_2(-x_2) = -u_2(x_2), \quad u_3(-x_2) = u_3(x_2). \tag{3.3}$$

However, $\partial u_1/\partial x_2|_w$ becomes undefined, and the filter operator does not commute with the derivative at the wall. As a result, Eq. (2.4) cannot be obtained.

The boundary conditions for the filtered velocity field are derived by consistency with the filter operator,

$$\bar{u}_i|_w = \mathcal{F}(u_i)|_w. \tag{3.4}$$

By construction of the extended velocity field (Eq. 3.1), the boundary conditions for the fNS equations reduce to the usual no-slip condition for the streamwise and spanwise filtered velocities

$$\bar{u}_1|_w = 0, \quad \bar{u}_3|_w = 0. \tag{3.5}$$

In the wall-normal direction, the condition that $\partial\bar{u}_2/\partial x_2|_w = 0$ is satisfied. However, evaluating the filtered continuity equation at the wall

$$\left.\frac{\partial\bar{u}_1}{\partial x_1}\right|_w + \left.\frac{\partial\bar{u}_2}{\partial x_2}\right|_w + \left.\frac{\partial\bar{u}_3}{\partial x_3}\right|_w = \left.\frac{\partial\bar{u}_2}{\partial x_2}\right|_w = 0, \tag{3.6}$$

and $\partial\bar{u}_2/\partial x_2|_w = 0$ does not contain any additional information. Thus, the proper boundary condition remains

$$\bar{u}_2|_w = \mathcal{F}(u_2)|_w. \tag{3.7}$$

Finally, the procedure to integrate $\bar{u}_i$ in time is outlined as follows:

1. Starting from an filtered velocity field, $\bar{u}_i$, and for a filter operator in integral form (Eq. 2.2), the three velocity components are extended following Eq. (3.1).
2. The unfiltered velocities, u_i, are obtained by reversing the filter, $u_i = \mathcal{F}^{-1}(\bar{u}_i)$.
3. The filtered Reynolds stress term, u_iu_j, is computed and filtered, $\overline{u_iu_j}$.
4. The filtered velocity field, $\bar{u}_i$, is advanced in time by integrating Eq. (2.4) with the boundary conditions in Eqs. (3.5) and (3.7).

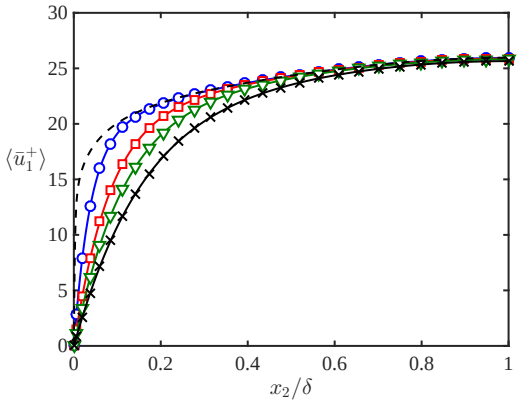

FIGURE 4. Filtered mean streamwise velocity profile for channel flow at $Re_\tau \approx 4200$. The filter operator is the differential filter (Eq. 2.8) with $a^2/\delta^2 = 0.001$ (circles), 0.005 (squares), 0.01 (triangles), and 0.02 (crosses).

Since the solution of the fNS equations (Eq. 2.4) is equivalent to the filtered solution of the NS equations (Eq. 2.1), the procedure above is not necessary, and it simply illustrates that the proposed method is well defined.

3.2. *A-priori results for channel flow*

In this section, we apply the extension method with the differential filter from Eq. (2.8) to DNS data of channel flow at $Re_\tau = u_\tau \delta/\nu \approx 4200$ (Lozano-Durán & Jiménez 2014), where δ is the channel half height, and u_τ is the friction velocity. The resulting $\langle \bar{u}_1 \rangle$ for various values of a^2 are plotted in Figure 4, where $\langle \cdot \rangle$ denotes averages in homogeneous directions and time. It is important to remark that the original flow can be reconstructed by reversing the filter, and the reconstructed flow collapses up to machine precision onto the original mean velocity profile. Also note that for an explicitly filtered LES consistent with the fNS equations, the predictions for the velocity profile aim to capture the filtered DNS quantities, unlike implicitly filtered LES, which is usually compared with the unfiltered DNS data.

4. Conclusions

The equations for LES are formally derived by low-pass filtering the NS equations with the effect of the small scales on the larger ones captured by a SGS model. However, it is known that the LES equations usually employed in practical applications are inconsistent with the filter operator when no explicit filter is used. Moreover, even for explicitly filtered LES, some inconsistencies remain in the wall-normal direction due to the constraining effect of the wall. A typically undesirable effect stemming from the inconsistency between LES and the fNS equations is that DNS data can not be used to aid SGS modeling.

We have proposed a form of the incompressible fNS equations for flows over flat walls in which the continuity equation, the filter operator, and the boundary condition at the wall are consistently formulated. The velocity fields were extended in the wall-normal direction with respect to the wall in order to remove the limitation on the support of the kernel in the near-wall region. This allowed for the filter size to remain constant in the entire domain, enabling commutation of the filter and differentiation operators, which

is essential for rigorously deriving fNS equations. The consistent fNS equations will be useful in future works to inform SGS models for explicitly filtered LES.

Acknowledgments

This work was supported by NASA under the Transformative Aeronautics Concepts Program, Grant #NNX15AU93A.

REFERENCES

Bose, S. T., Moin, P. & You, D. 2010 Grid-independent large-eddy simulation using explicit filtering. *Phys. Fluids* **22**, 105103.

Carati, D., Winckelmans, G. S. & Jeanmart, H. 2001 On the modelling of the subgrid-scale and filtered-scale stress tensors in large-eddy simulation. *J. Fluid Mech.* **441**, 119–138.

Cardesa, J. I., Vela-Martín, A., Dong, S. & Jiménez, J. 2015 The temporal evolution of the energy flux across scales in homogeneous turbulence. *Phys. Fluids* **27**, 111702.

De Stefano, G. & Vasilyev, O. V. 2002 Sharp cutoff versus smooth filtering in large eddy simulation. *Phys. Fluids* **14**, 362–369.

Germano, M. 1986 Differential filters for the large eddy numerical simulation of turbulent flows. *Phys. Fluids* **29**, 1755–1757.

Gullbrand, J. & Chow, F. K. 2003 The effect of numerical errors and turbulence models in large-eddy simulations of channel flow, with and without explicit filtering. *J. Fluid Mech.* **495**, 323–341.

Kravchenko, A. G. & Moin, P. 2000 Numerical studies of flow over a circular cylinder at $Re_d = 3900$. *Phys. Fluids* **12**, 403–417.

Leonard, A. 1975 Energy cascade in large-eddy simulations of turbulent fluid flows. *Adv. Geophys.* **18**, 237–248.

Leonard, A. 1997 Large-eddy simulation of chaotic convection and beyond. *AIAA Paper* #97-0204.

Lozano-Durán, A. & Jiménez, J. 2014 Effect of the computational domain on direct simulations of turbulent channels up to $Re_\tau = 4200$. *Phys. Fluids* **26**, 011702.

Lund, T. S. 2003 The use of explicit filters in large eddy simulation. *Comput. Math. App.* **46**, 603–616.

Meyers, J. & Sagaut, P. 2007 Is plane-channel flow a friendly case for the testing of large-eddy simulation subgrid-scale models? *Phys. Fluids* **19**, 048105.

Stolz, S., Adams, N. A. & Kleiser, L. 2001 An approximate deconvolution model for large-eddy simulation with application to incompressible wall-bounded flows. *Phys. Fluids* **13**, 997–1015.

Vasilyev, O. V., Lund, T. S. & Moin, P. 1998 A general class of commutative filters for LES in complex geometries. *J. Comput. Phys.* **146**, 82–104.

Winckelmans, G. S., Wray, A. A., Vasilyev, O. V. & Jeanmart, H. 2001 Explicit-filtering large-eddy simulation using the tensor-diffusivity model supplemented by a dynamic smagorinsky term. *Phys. Fluids* **13**, 1385–1403.

Yeo, W. K. 1987 *A generalized high pass/low pass averaging procedure for deriving and solving turbulent flow equations*. Ph.D. Thesis, The Ohio State University.